Dependence of lung injury on inflation rate during low-volume ventilation in normal open-chest rabbits

EDGARDO D'ANGELO[1], MATTEO PECCHIARI[1], MARINA SAETTA[2], ELISABETTA BALESTRO[2], JOSEPH MILIC-EMILI[3]

[1]Istituto di Fisiologia Umana I, Università di Milano, 20133 Milan, Italy, Dipartimento di Medicina Clinica e Sperimentale, Università di Padova, 35128 Padua, Italy, and Meakins-Christie Laboratories, McGill University, Montreal, Quebec, Canada H2X 2P2

Running title: LOW-VOLUME VENTILATION

Address correspondence to:
Edgardo D'Angelo, MD
Istituto di Fisiologia Umana I
via Mangiagalli 32
20133 Milan, Italy
Tel. +39-02-50315440; Fax +39-02-50315430
E-mail edgardo.dangelo@unimi.it

ABSTRACT

Lung mechanics and morphometry were assessed in two groups of 9 normal open-chest rabbits mechanically ventilated (MV) for 3-4 h at zero end-expiratory pressure (ZEEP) with physiologic tidal volumes (V_T=11 ml·kg^{-1}) and high (*group A*) or low (*group B*) inflation flow (44 or 6.1 ml·kg^{-1}·s^{-1}). Relative to initial MV on PEEP (2.3 cmH_2O), MV on ZEEP increased quasi-static elastance (Est), airway (Rint) and viscoelastic resistance (Rvisc) more in *group A* (+251, +393, and +225%, respectively) than B (+180, +247, and +183%, respectively), with no change in viscoelastic time constant. After restoration of PEEP, Est and Rvisc returned to control, whilst Rint, still relative to initial values, remained elevated more in *group A* (+86%) than *B* (+33%). In contrast, prolonged high flow MV on PEEP had no effect on lung mechanics of 7 open-chest rabbits (*group C*). Gas exchange on PEEP was equally preserved in all groups and the lung wet/dry ratios were normal. Relative to *group C*, both *group A* and *B* had an increased percentage of abnormal alveolar-bronchiolar attachments and number of polymorphonuclear leukocytes in alveolar septa, the latter being significantly larger in *group A* than *B*. Thus, prolonged MV on ZEEP with cyclic opening-closing of peripheral airways causes alveolar-bronchiolar uncoupling and parenchymal inflammation with concurrent, persistent increase in Rint, that are worsened by high inflation flow.

keywords: lung mechanics, viscoelasticity, recruitment-derecruitment of lung units, airway-parenchymal coupling, parenchymal inflammation

In an *ex vivo* model of lavaged rat lung, Muscedere et al. (16) showed that ventilation with physiologic tidal volumes from zero end-expiratory pressure (ZEEP) resulted in a significant increase of histologic injury scores in the respiratory and membranous bronchioles relative to ventilation from positive end-expiratory pressure (PEEP) above the lower inflection point on the static inflation volume-pressure curve of the lung. Subsequently, it has been shown that also in normal open-chest rabbits prolonged (3-4 h) mechanical ventilation at ZEEP induces histological evidence of peripheral airway injury with a concomitant increase in airway resistance which persists after restoration of physiological end-expiratory lung volume (9). In this study, morphological and mechanical alterations have been attributed to shear stresses caused by cyclic opening and closing of peripheral airways with tidal ventilation at low lung volumes, as previously suggested by Robertson (17), possibly combined with increased surface tension due to surfactant depletion or inactivation. Furthermore, it was also observed that during the first 90 ms of inflation the transpulmonary pressure increased five-fold more rapidly during ventilation at ZEEP than with PEEP, in spite of equal inflation flows under the two conditions. This suggests that the higher increase of transpulmonary pressure at the onset of inflation may contribute to lung injury on ZEEP.

Accordingly, in the present study we have assessed in normal, anesthetized, paralyzed, open-chest rabbits the effects of different inflation rates during low lung volume ventilation for 3-4 h on *a)* lung mechanics; and *b)* histologic indices of lung injury and inflammation.

METHODS

Twentyfive New Zeeland white rabbits (weight range 2.2-3.1 kg) were anesthetized with an intravenous injection of a mixture of pentobarbital sodium (20 $mg \cdot kg^{-1}$) and urethane (0.5 $mg \cdot kg^{-1}$). A brass cannula and a polyethylene catheter were inserted into the trachea and carotid artery, respectively. The animals were paralyzed with pancuronium bromide (0.1 $mg \cdot kg^{-1}$) and mechanically ventilated (respirator 660; Harvard Apparatus, Holliston, MA) with a pattern similar to that during spontaneous breathing. Anesthesia and complete muscle relaxation were maintained with additional doses of the anesthetic mixture and pancuronium bromide. Adequateness of anesthesia was judged from the absence of mydriasis, sudden increase in heart rate and/or systemic blood pressure. The chest was opened via a median sternotomy and a coronal cut made just above the costal arch. Application of positive end-expiratory pressure (PEEP) of 2-2.5 cm H_2O prevented lung collapse.

Airflow (V') was measured with a heated Fleisch pneumotachograph no.00 (HS Electronics, March-Hugstetten, Germany) connected to the tracheal cannula and a differential pressure transducer (Validyne MP45, ±2 cm H_2O; Northridge, CA). The response of the pneumotachograph

was linear over the experimental range of V'. Tracheal pressure (Ptr) and systemic blood pressure were measured with pressure transducers (model 1290A; Hewlett-Packard, Palo Alto, CA) connected to the side arm of the tracheal cannula and carotid catheter, respectively. There was no appreciable shift in the signal or alteration in amplitude up to 20 Hz. The signals from the transducers were amplified (model RS3800; Gould Electronics, Valley View, OH), sampled at 200 Hz by a 14-bit A/D converter, and stored on a desk computer. Volume changes (ΔV) were obtained by numerical integration of the digitized airflow signal. Arterial blood P_{O_2}, P_{CO_2} and pH were measured by means of a blood gas analyzer (IL 1620; Instrumentation Laboratory, Milan, Italy) on samples drawn at the beginning and at the end of each test session.

After completion of the surgical procedure, the rabbits were ventilated with a specially designed, computer-controlled ventilator, delivering water-saturated air from a high pressure source (4 atm) at constant flow of different selected magnitudes and durations. The inspiratory and expiratory solenoid valves (model S50 and S80; Peter Paul, New Britain, CT) had a closing or opening time of 5 ms: they could be also used to occlude the airways either at end-inspiration or end-expiration for 5 s. The inspiratory and expiratory valves were connected to the pneumotachograph attached to the tracheal cannula by means of short rigid tubings. A Fleisch pneumotachograph (no.00) connected to the exhaust valve (model S50) of the inspiratory line and differential pressure transducer (Validyne MP45, ±2 cm H_2O) provided the feedback signal to the computer for the fine adjustement of the proportional valve (model PSV1; Aalborg, Orangeburg, NY) setting the inflation flow. A three way stopcock allowed the connection of the expiratory valve either to the ambient or to a drum in which the pressure was set at 2.0-2.5 cm H_2O by means of a flow-through system.

Two groups of nine and seven rabbits, respectively, were ventilated with high inflation flow (*groups A* and *C*) and nine rabbits (*group B*) with low inflation flow. In all instances the baseline ventilator settings consisted of fixed tidal volume (V_T; 11 $ml \cdot kg^{-1}$) and cycle duration (T_{TOT}) of 3 s, whilst the inspiratory duration (T_I) was 0.25 for *group A* and *C* and 1.8 s for *group B*, respectively (Fig. 1). In *groups A* and *C*, an end-inspiratory pause of 0.75 s was applied in order to ensure the same mean lung volume during the respiratory cycle for all groups. During baseline ventilation, the inflation flow and T_I/T_{TOT} were 44 $ml \cdot kg^{-1} \cdot s^{-1}$ and 0.33 for *group A* and *C*, and 6.1 $ml \cdot kg^{-1} \cdot s^{-1}$ and 0.6 for *group B*, respectively. With the above settings, no intrinsic PEEP was present under any experimental condition, as evidenced by an end-expiratory pause (zero flow) and absence of Ptr changes with airway occlusion at end-expiration. During the measurements, the ribs on the two sides and the diaphragm were pulled widely apart, in order to prevent contact between lung and chest wall, except in their dependent parts.

Procedure and data analysis

Measurements of lung mechanics were performed as previously described (9). Briefly, with the baseline ventilator settings kept constant, *group A* and *B* rabbits were subjected to the following sequence of PEEP and ZEEP: *a)* 15 min of mechanical ventilation (MV) with PEEP ($PEEP_1$); *b)* 3-4 h of MV at ZEEP; *c)* 15 min of MV with PEEP ($PEEP_2$). Lung mechanics was assessed with the rapid airway occlusion method (3,6) during the $PEEP_1$ and $PEEP_2$ periods, and after about 10 min ($ZEEP_1$) and at the end of the ZEEP period ($ZEEP_2$). Ten to fifteen min elapsed between measurements on $ZEEP_2$ and $PEEP_2$. In *group C* rabbits, which were ventilated as those of *group A* but only on PEEP, assessment of lung mechanics was made 5-10 min after the onset of MV with PEEP ($PEEP_1$) and at the end of the 3-4 h PEEP period ($PEEP_2$). Before all measurements on PEEP the lungs were inflated 3-4 times to Ptr of ~25 cm H_2O. Two types of measurements were carried out: *a)* while keeping V_T at baseline values, test breaths were intermittently performed with different V'_I and T_I in the range 0.25 to 3 s to assess lung mechanics at end-inflation; and *b)* while keeping V'_I at baseline values, test breaths were intermittently performed with different V_T to obtain quasi-static inflation volume-pressure curves. End-inspiratory occlusions lasting 5 s were made in all test breaths, which were performed in random order and repeated 4-5 times under all experimental conditions. During ventilation at ZEEP, end-inspiratory occlusions were performed only for tidal volumes ≤ baseline V_T. During ventilation with PEEP, the expiratory valve was opened to the ambient for 4-6 expirations in order to measure the difference between the end-expiratory and the resting lung volume (ΔEELV); these breaths were followed by two inflations with Ptr of 20-25 cm H_2O. The animals were from a single cohort and the experiments were done in random order.

The end-inspiratory airway occlusions were followed by a rapid initial drop in Ptr (ΔP_1), and by a slow decay (ΔP_2) to an apparent plateau value (Pst). This pressure, computed as the mean pressure recorded during the last 0.5 s of occlusion, was taken to represent the quasi-static lung recoil pressure, while ΔP_1 and ΔP_2 divided by V'_I yielded the lung interrupter (Rint) and additional (ΔR) resistances, respectively. Viscoelastic parameters, Rvisc and $\tau visc = Rvisc/Evisc$, were computed by fitting the values of ΔR and T_I with the function (7)

$$\Delta R = Rvisc \cdot (1 - e^{-T_I/\tau visc}) \quad (1)$$

while lung quasi-static elastance (Est) was obtained as $(Pst-Pee)/V_T$, Pee being the end-expiratory pressure. After completion of the mechanics measurements, the left lung was processed for histological analysis, while the right lung was weighed immediatedly after removal, left overnight in an oven at 120 °C, and weighed again to compute the wet/dry ratio.

Histological analysis

Lung fixation was performed in seven animals of *group A* and *B*, respectively, and in five animals of *group C*. The rabbits were given heparin (355 U/kg) and papaverin (5 mg/kg) intravenously to prevent bronchospasm. The pericardium was removed, ties were placed around the descending aorta and the hilum of the right lung, and a large needle was inserted through the right ventriculum into the pulmonary artery. After three inflations to 25 cmH_2O, the transpulmonary pressure was kept at 10 cmH_2O, the ties were fastened, the right lung was removed, the right atrium cut, and the left lung perfused with saline until the lobar surfaces became white. Thereafter, lung fixation was obtained by perfusing with 4% formaldehyde, 0.1% glutardialdehyde dissolved in 0.12 M phosphate buffer. Six blocks, 1cm thick, involving both subpleural and para-hilar regions, were obtained in each animal. Each block was processed through a graded series of alcohols and embedded in paraffin. From each block, sections of 5 μm thickness were cut and stained with hematoxylin-eosin for light miscroscopy analysis. Histologic evaluation was performed by a single observer who had no knowledge of the mechanical data. The following measurements were obtained: *a)* mean linear intercept (Lm), which is a measure of airspace enlargement, as described by Thurlbeck (26); *b)* indexes of destruction of the alveolar attachments, which are the alveolar walls that extend radially from the outer wall of the non respiratory bronchioles (19); and *c)* polymorphonuclear leukocytes count in the alveolar walls, which is an index of parenchymal inflammation (20).

For Lm measurements, one section from each block was examined at a magnification of 125X, and 40 non-overlapping fields were analyzed on each section, giving a total of 240 fields per animal. The value of Lm was obtained as the ratio between the length in μm of a line passing transversely through each field and the number of alveolar walls intercepting that line, the final result for a given animal being the average Lm of the 240 fields examined.

For alveolar-bronchiolar coupling evaluation, the percentage of abnormal alveolar attachments and the distance between attachments were assessed in 50 non respiratory bronchioles per animal. Any discontinuity or rupture of the alveolar walls was considered an abnormality, and such alveolar walls were called abnormal attachments. In each airway, peribronchiolar alveolar walls (normal and abnormal attachments) were counted directly in the microscopic field at a magnification 250X. The external circumference was measured using a computer–aided image analysis (Casti Imaging, Venice, Italy). Two indexes were obtained for *group A* and *B*: a) abnormal attachments computed as the percent ratio of abnormal to total (normal and abnormal) attachments; and b) distance between normal attachments (μm) computed as the ratio of external circumference to number of normal attachments, whilst for *group C* only the former index was assessed.

Inflammatory cell counts in the lung parenchyma were performed as previously described (20). Briefly, at a magnification 800X the number of polymorphonuclear leukocytes within the alveolar wall was computed and the length of the alveolar wall was measured. Ten fields randomly distributed across the slide were studied, and the result was expressed as number of polymorphonuclear leukocytes/mm of alveolar wall. For each animal a total of 60 fields were examined.

Statistics. Results from mechanical studies are presented as means±SE. The least-square regression method was used to assess the parameters in *Eq. 1* and of the pressure-volume relationship of the lungs. Comparisons among experimental conditions were performed using one-way analysis of variance (ANOVA); when significant differences were found, the Bonferroni test was performed to determine significant differences between different experimental conditions. Results from histologic studies are expressed as median and range, and the statistical analysis was performed using the Mann-Whitney test. The level for statistical significance was taken at $P \leq 0.05$.

RESULTS

Ventilation on PEEP

In each animal, the values of Pa_{O_2}, Pa_{CO_2}, and pHa obtained at the beginning and at the end of the $PEEP_1$, $ZEEP_1$, $ZEEP_2$, and $PEEP_2$ sessions did not differ significantly and were thus averaged. The mean values of these parameters during $PEEP_1$ and $PEEP_2$, and the wet-to-dry ratio assessed at the end of the experiments were similar for all groups of rabbits (Table 1). The values of wet-to-dry ratio were similar to those of freshly excised rabbits lungs (9).

Owing to the higher inflation flow, the mean rate of Ptr changes during the first 90 ms of inflation ($\Delta P/\Delta t$) with $PEEP_1$ was about 7 fold larger in *groups A* and *C* than *B* (Table 2). Relative to $PEEP_1$, $\Delta P/\Delta t$ increased significantly with $PEEP_2$ in both *groups A* and *B*, whilst it remained unchanged in *group C*.

Static V-P relationships. In all groups of rabbits the end-expiratory pressure was almost the same during $PEEP_1$ and $PEEP_2$, averaging 2.3±0.1 cm H_2O. Similarly, in all groups the mean values of ΔEELV did not differ significantly among the various conditions (Table 3). In all animals, independent of ventilation on ZEEP, the inflation V-P curve on PEEP closely fitted (r>0.95) a function in the form $V_o \cdot (1-e^{-K \cdot Pst},)$, where V_o is maximum volume above resting lung volume and K=cm H_2O^{-1} is a shape factor, that reflects the overall distensibility of the lung (5,21). The mean values of these constants are reported in Table 3. Because the values of V_o and K did not change in all animals after prolonged ventilation on ZEEP (*groups A* and *B*) or PEEP (*group C*), a unique

relationship could be used to describe the quasi-static V-P curve above the end-expiratory lung volume with PEEP, as shown in Fig. 2.

Elastance. On the basis of the V_o and ΔEELV values in Table 3, tidal ventilation with PEEP occurred in the range 33-67% V_o. The group mean values of Est obtained under the various conditions are reported in Table 4. None of these values differed significantly between $PEEP_1$ and $PEEP_2$ (P=0.094).

Rint. During the end-inspiratory occlusions at baseline V_T, Rint was independent of flow, at least in the range 10-100 $ml \cdot s^{-1}$, in all animals and conditions; hence the values of Rint obtained in each rabbit and condition were averaged (Table 4). With $PEEP_1$, Rint did not differ significantly among the three groups of animals. With $PEEP_2$, Rint increased significantly relative to $PEEP_1$ in all animals of *group A*, and in five animals of *group B*. On average, Rint was significantly increased in both groups of rabbits by 86±12 and 39±12%, respectively, but the increase was significantly larger in *group A* (12±0.2 vs 6±0.1 $cmH_2O \cdot s \cdot l^{-1}$; $P<0.001$). In *group C*, the prolonged ventilation on PEEP, *i.e.* from $PEEP_1$ to $PEEP_2$, caused a significant increase of Rint in one animal and a significant decrease in another animal, but the group mean value of Rint was almost unchanged (Table 4).

Viscoelastic properties. In all animals and conditions, a unique function in the form of *Eq. 1* adequately described the experimental ΔR-T_I data ($r>0.94$), allowing computation of Rvisc and τvisc. Figure 3 depicts the group mean relationships of ΔR to T_I obtained under the various experimental conditions. With $PEEP_2$, neither Rvisc nor τvisc changed significantly relative to corresponding $PEEP_1$ values in all groups of rabbits (Table 5). On an individual basis, Rvisc was, however, increased significantly in four and two animals of *group A* and *B*, respectively. No significant changes of either Rvisc or τvisc were observed in any animal of *group C*.

Ventilation on ZEEP

Relative to $PEEP_1$, with $ZEEP_1$ there was a similar increase of Pa_{CO_2} and decrease of Pa_{O_2} and pHa both in *group A* and *B* (Table 1). With further ventilation on ZEEP ($ZEEP_2$), there was a small but significant increase of Pa_{O_2}, while pHa and Pa_{CO_2} remained essentially unchanged (Table 1). Since this occurred in both *group A* and *B*, the values of Pa_{O_2}, Pa_{CO_2} and pHa were similar among the animals of the two groups also with $ZEEP_2$.

The average values of $\Delta P/\Delta t$ increased markedly on ZEEP both in *group A* and *B*, and a further significant increase occurred with prolonged ventilation on ZEEP (Table 2).

Elastance. According to the V_O values in Table 3, baseline tidal ventilation on ZEEP occurred in the range of 0 to 33% V_O. There was both an immediate and a progressive increase in Est with ventilation on ZEEP (Table 4), both in animals ventilated with high (*group A*) and low inflation flows (*group B*). These changes were, however, significantly larger in *group A* than *B*, both at $ZEEP_1$ (250±17 *vs* 185±13 $cmH_2O \cdot l^{-1}$; $P<0.001$) and $ZEEP_2$ (328±14 *vs* 258±6 $cmH_2O \cdot l^{-1}$; $P<0.001$). Moreover the quasi-static V-P relationship, which on PEEP was slightly concave towards the pressure axis, became sigmoidal (Fig. 2). While Est on PEEP was significantly lower than that at baseline V_T for any tidal volume below baseline V_T, on ZEEP it was significantly larger than that at baseline V_T with tidal volumes of 4.4 and 8.9 ml (ΔEst=11.7±1.6 and 5.3±1.1 $cmH_2O \cdot l^{-1}$, respectively; $P<0.001$), and lower with a tidal volume of 18 ml (ΔEst=-4.7±0.9 $cmH_2O \cdot l^{-1}$; $P<0.001$).

Rint. The mean values of Rint obtained on $ZEEP_1$ and $ZEEP_2$ during ventilation with high and low inflation flows are shown in Table 4. In both groups of animals, there was an immediate and a progressive increase of Rint. With $ZEEP_1$, the increase of Rint, relative to that with $PEEP_1$, amounted to 148±16 and 63±10% in *group A* and *group B*, while with $ZEEP_2$ and relative to $PEEP_2$, it amounted to 177±25 and 157±25% in the two groups of rabbits, respectively. Hence, there was a significant increase of Rint with prolonged ventilation on ZEEP both in animals ventilated with high and low inflation flows, but the increase in Rint was significantly larger in *group A* than *group B*, both on $ZEEP_1$ (20±2 vs 9±1 $cmH_2O \cdot s \cdot l^{-1}$; $P<0.001$) and $ZEEP_2$ (55±7 vs 36±5 $cmH_2O \cdot s \cdot l^{-1}$; $P=0.022$).

Viscoelastic properties. Figure 3 depicts the relationships of ΔR to T_I pertaining to *group A* and *B* obtained with $ZEEP_1$ and $ZEEP_2$, the group mean values of Rvisc and τvisc being reported in Table 5. Both Rvisc and τvisc did not differ significantly between the two groups of animals under any conditions. With $ZEEP_1$, Rvisc increased significantly relative to that with PEEP1 in *group A* (ΔRvisc=97±24 $cmH_2O \cdot s \cdot l^{-1}$; $P<0.001$) and *B* (ΔRvisc=58±12 $cmH_2O \cdot s \cdot l^{-1}$; $P<0.001$), and a further significant increase occurred between $ZEEP_1$ and $ZEEP_2$ in *group A* (ΔRvisc=29±9 $cmH_2O \cdot s \cdot l^{-1}$; $P<0.001$) and *B* (ΔRvisc=50±15 $cmH_2O \cdot s \cdot l^{-1}$; $P<0.001$). In contrast, τvisc remained essentially the same under all conditions. The effects of ZEEP on Rvisc were qualitatively similar to those of Est reported above (Table 4). Indeed, there was a highly significant correlation between changes in Est and Rvisc, both expressed relative to the corresponding values during $PEEP_1$, observed in all animals with $ZEEP_1$ and $ZEEP_2$ (Fig. 4).

Histology

Figure 5 illustrates the infiltration of polymorphonuclear leukocytes that occurred in the alveolar septa of rabbits ventilated on ZEEP with high or low inflation flows (right and left panel, respectively), while figure 6 shows the different degrees of airway-parenchyma uncoupling as it could be inferred from the presence of abnormal alveolar-bronchiolar attachments. The results of measurements of airspace enlargement (Lm), peribronchiolar alveolar wall destruction (% abnormal attachments, distance between normal attachments), and cell counts in the lung parenchyma (cells/mm of alveolar wall) are shown in Table 6 for all groups of rabbits. The values of Lm, percentage of abnormal attachments and distance between normal attachments were similar in *group A* and *B*. When parenchymal inflammation was analysed, the number of polymorphonuclear leukocytes within the alveolar wall was significantly larger in *group A* than *B* (P=0.018). On the other hand, both the number of polymorphonuclear leukocytes within the alveolar wall and the percentage of abnormal alveolar-bronchiolar attachments were markedly smaller in *group C*, while the values of Lm were essentially the same in all groups (Table 6). No signs of focal alveolar collapse, edema, hemorrhages, and epithelial desquamation in alveoli (24) were present in all groups of rabbits.

DISCUSSION

Lung injury during ventilation at low lung volumes with physiologic tidal volumes is generally attributed to cyclic opening and closing of relatively small airways with concomitant generation of abnormal, inhomogeneous shear stresses that are eventually responsible for mechanical and histological damage in respiratory and membranous bronchioles with a concurrent increase in airway resistance (9,16). The present results indicate that the increase in airway resistance is associated with an inflammatory response and marked alterations of alveolar-bronchiolar coupling, and that the inflammatory reaction is substantially augmented by the use of high inflation flows. On the other hand, when lung volumes are kept within the physiological range with PEEP, prolonged ventilation with high inflation flows does not cause mechanical changes, while essentially no damage of alveolar-bronchiolar attachments and signs of inflammatory reaction are observed.

In line with previous results (9), during mechanical ventilation with PEEP there was no evidence of airway closure since the static inflation V-P curve of the lung was concave to the pressure axis, as shown in Figure 2 (11). In contrast, at ZEEP the inflation V-P curve became sigmoidal, its initial part being convex to the pressure axis, reflecting progressive reopening of small airway (<1mm in diameter) (12). Thus, during mechanical ventilation on ZEEP there was cyclic airway

opening and closing, which should be responsible for the observed histological alterations as well as the increase in Rint on PEEP2 relative to PEEP1. Moreover, the convexity of the initial part of the quasi-static inflation V-P curve on ZEEP was more pronounced in animals ventilated with high inflation flow (Fig. 2), the ratio between Est with the lowest inflation volume (~4 $ml \cdot kg^{-1}$) and baseline VT being significantly larger in *group A* than *B* (1.34±0.06 vs 1.18±0.05; P=0.032). This suggests that during ventilation with high inflation flow more airways were involved in cyclic opening and closing with concurrent greater mechanical and histological damage (Tables 4 and 6).

On ZEEP, both in *group A* and *B*, there was a significant increase of Est, Rint, and Rvisc relative to PEEP1, which was significantly greater after 3-4 h (ZEEP2) than after 5-10 min (ZEEP1) of ventilation on ZEEP (Tables 4 and 5). Similar results have been obtained in a previous study on open-chest rabbits ventilated with inflation flows (~9 $ml \cdot kg^{-1} \cdot s^{-1}$), which were close to those of *group B* (9). A progressive increase of total lung resistance and dynamic elastance during mechanical ventilation at low lung volumes has been previously reported in normal open-chest rabbits (25).

Two mechanisms may account for the increase of Est and Rvisc that occurs on ZEEP relative to PEEP, as well as for their progressive increase with time, namely an increase of lung stiffness due to larger surface forces, and a decrease of ventilated tissue caused by airway closure and/or alveolar collapse. An increase of surface forces with time at low end-expiratory transpulmonary pressure and lung volume has been advocated to explain the changes of lung compliance in the absence of detectable airway closure (29,30). It could also explain the increase in Rvisc, especially on ZEEP2, since most of Rvisc should reside in the air-liquid interface (2). A reduction in ventilated tissue due to airway closure or alveolar collapse should cause proportional changes of Est and Rvisc, while leaving τvisc unaffected, as was in fact the case (Tables 4 and 5, and Fig. 4). Based on theoretical considerations, diffuse alveolar collapse has been predicted to take place at low lung volumes (22,23), but visible areas of atelectasis did not occur in the present animals. Accordingly, it is likely that increased surface tension and small airway closure are the main mechanisms leading to increased Est and Rvisc during ventilation on ZEEP, with a possible contribution from microatelectasis. Persistent small airway closure and dependent air trapping should have been evenly distributed throughout the lung, because on visual inspection lung expansion in both *group A* and *B* was apparently uniform on ZEEP as on PEEP. Hence, overdistension of recruited lung units on ZEEP was likely similar during ventilation with low and high inflation flow, or even smaller under the latter condition, if more airways were involved in cyclic opening and closing (see above).

The increase in airway resistance with acute reductions in lung volume has been ascribed to the concomitant decrease in lung recoil (13). Under the present conditions, however, the lung recoil at baseline VT (*i.e.* the lung volume at which Rint was assessed) was larger during ZEEP than PEEP, and

larger on ZEEP2 than ZEEP1 (Fig. 2), whilst Rint was larger on ZEEP than on PEEP, and larger on ZEEP2 than ZEEP1 (Table 4). The increase in Rint was not due to the changes in arterial blood gases or pH with ZEEP (Table 1), hypercapnia and acidosis observed on ZEEP having, if any, a bronchodilating effect (8). Moreover, hypercapnic acidosis has been reported to exert a protective effect on ventilator induced lung injury (4). The increase in Rint should be instead related to *a)* reduction of ventilated tissue due to small airway closure; *b)* uncoupling between peripheral airways and lung parenchyma, as suggested by the occurrence of a large number of abnormal alveolar attachments and increased distance between attachments (Table 6), such that the airway caliber was reduced in spite of increased lung recoil; and *c)* increased bronchomotor tone due to release of inflammatory mediators, as indicated by the presence of polymorphonuclear leukocytes (Table 6). Since the number of abnormal alveolar attachments and the distance between attachments were not significantly different between *group A* and *B*, and the amount of gas trapping possibly larger in *group B*, the greater increase of Rint on ZEEP with high inflation flow was probably due to a greater contribution of mechanisms *c*.

After return of *group A* and *B* rabbits to PEEP (PEEP2), Rvisc as well as Est reversed to the initial (PEEP1) values (Tables 4 and 6), while Rint remained significantly ($P<0.001$) larger (Table 4). The increase in Rint on PEEP2 could not be related to changes in arterial blood gases or pH, as the latter were not significant (Table 1), or to changes in the elastic recoil, since the quasi-static V-P curve, as well as Est, were almost the same on PEEP1 and PEEP2 in all groups of rabbits (Fig. 1 and Table 4). Absence of parenchymal alterations was further indicated by the Lm values (Table 6) that were similar to those of *group C* rabbits and within the range of those obtained in normal rabbits lung at corresponding distending pressure (5). Hence, the increase in Rint with PEEP2 was due to changes in the mechanical coupling between peripheral airways and lung parenchyma, as reflected by abnormal alveolar attachments and increased distance between attachments, and increased bronchomotor tone with release of mediators by inflammatory cells (Table 6). Indeed, both the percentage of abnormal attachments and the number of inflammatory cells in the alveolar septa were markedly larger in *groups A* and *B* than *C*, which did not exhibit any significant change in Rint from PEEP1 to PEEP2 (Tables 4 and 6). Finally, the increased Rint could have also been in part related to changes in the mechanical properties of the peripheral airways themselves, since in normal open-chest rabbits evidence of peripheral airway injury, with epithelial necrosis and sloughing, have been found after prolonged ventilation on ZEEP in lungs that were fixed by intra-tracheal infusion of formalin at a distending pressure of 20 cm H_2O (9).

The increase in Rint between PEEP1 and PEEP2 was markedly larger in *group A* than *B* (Table 4). Assuming that the increase of Rint was due to peripheral airway resistance (9) and that under

normal conditions peripheral airway resistance (Rp) contributes 20% of Rint (13), Rp with PEEP1 should have amounted to about 3 $cmH_2O \cdot s \cdot l^{-1}$ in all groups of animals, and the increase with PEEP2 to about 15 and 8 $cmH_2O \cdot s \cdot l^{-1}$ in *group A* and *B*, respectively. Compared to ventilation with low inflation flows (*group B*), ventilation with high inflation flow, and hence higher $\Delta P/\Delta t$ (Table 2), should have caused larger stresses in the lung parenchyma surrounding occluded airways (14). Moreover, opening of small airways with rapid inflations could have required pressures substantially larger than critical pressures, due to latent opening time (1). This could have in turn produced a more marked disruption of the mechanical linkage between parenchyma and small airways, as well as more pronounced alveolar epithelial cell injury (27,28) with inflammatory reaction and release of brochomotor mediators. The present results (Table 6) indicate that the latter mechanisms was the main cause of the larger increase in Rint during low-volume ventilation with high inflation flows.

Recruitment of polymorphonuclear leukocytes in the alveolar walls during low-volume ventilation and their greater increase with high inflation flows should be of interest in connection with a recently described type of ventilator-induced lung injury called *biotrauma* (10). Parenchymal overdistension and shear forces generated during repetitive opening and closure of lung units can exacerbate or even initiate significant lung injury and inflammation. However, the relationship among mechanical stimuli, lung injury, and cellular inflammatory response is not fully understood. In particular, the interaction between inflammatory cells and structural cells in the pathogenesis of lung injury has not yet been clarified. There is evidence that mechanical ventilation can lead to release of mediators that prime polymorphonuclear leukocytes, which may represent the major effector cells in the generation of tissue injury, especially considering their potential interaction with other candidate cells, such as alveolar epithelial cells, an additional potential source of inflammatory mediators, contributing to the upregulation of the inflammatory response (10,27). The finding of an increased number of polymorphonuclear leukocytes within the alveolar walls suggests that the interaction between these inflammatory cells and alveolar epithelial cells could play a crucial role in the pathogenesis of ventilator-induced lung injury.

In the present open-chest rabbits, histologic lesions and signs of inflammation were found throughout the lungs because pleural surface pressure was essentially uniform. With closed-chest, however, the lesions should be mainly located in the dependent lung zones, where airway closure occurs preferentially because of lower transpulmonary pressure (15). In this condition, breathing with high inspiratory flows causes redistribution of the inspired volume towards the dependent regions (18), likely increasing the number of airways subjected to cyclic opening and closing, as well as the stress exerted by the expanding parenchyma on closed airways. Based on the present

results, it seems likely that also with closed chest the mechanical and histological damage in the dependent lung zones should be greater with rapid than slow inspirations.

In conclusion, the present study confirms our previous results in normal, open-chest rabbits (9) that after 3-4 h of mechanical ventilation at low lung volume, there is an increase of airway resistance (Rint), which persists after restoration of normal end-expiratory volumes. In addition, the present results show that this increase in Rint is associated with alteration of alveolar-bronchiolar coupling and lung inflammation, as reflected by the number of polymorphonuclear leukocytes in the alveolar septa, and that the latter effects is greater with fast than slow lung inflations.

REFERENCES

1. Allen G, Lundblad LKA, Parson P, and Bates JHT. Transient mechanical benefits of a deep inflation in the injured mouse lung. *J Appl Physiol* 93: 1709-1715, 2002.
2. Bachofen H, Hildebrandt J, and Bachofen M. Pressure-volume curves of air- and liquid-filled excised lungs - surface tension in situ. *J Appl Physiol* 29: 422-431, 1970.
3. Bates JHT, Bacconier P, and Milic-Emili J. A theoretical analysis of interrupter technique for measuring respiratory mechanics. *J Appl Physiol* 64: 2204-2214, 1988.
4. Broccard AF, Hotchkiss JR, Vannay C, Markert M, Sauty A, Feihl P, Schaller MD. Protective effects of hypercapnic acidosis on ventilator-induced lung injury. *Am J Respir Crit Care Med* 164: 8002-806, 2001.
5. D'Angelo E. Local alveolar size and transpulmonary pressure in situ and in isolated lungs. *Resp.Physiol.* l4: 251-266, 1972.
6. D'Angelo E. Stress-strain relationships during uniform and non-uniform expansion of isolated lungs. *Respir Physiol* 23: 87-107. 1975.
7. D'Angelo E, Calderini E, Torri G, Robatto FM, Bono D, and Milic-Emili J. Respiratory mechanics in anesthetized paralyzed humans: effects of flow, volume, and time. *J Appl Physiol* 67: 2556-2564, 1989.
8. D'Angelo, E., I. Salvo Calderini and M. Tavola. The effects of CO_2 on respiratory mechanics in normal anesthetized paralyzed humans. *Anesthesiology* 94: 604-610, 2001.
9. D'Angelo E, Pecchiari M, Baraggia P, Saetta M, Balestro E, and Milc-Emili J. Low-volume ventilation causes peripheral airway injury and increased airway resistance in normal rabbits. *J Appl Physiol* 92: 949-956, 2002.
10. Dos Santos CC, and Slutsky AS. Cellular responses to mechanical stress. Invited Review: Mechanisms of ventilator-induced lung injury: a perspective. *J Appl Physiol* 89: 1645-1655, 2000.
11. Glaister DH, Schroter RC, Sudlow MF, and Milic-Emili J. Transpulmonary pressure gradient and ventilation distribution in excised lungs. *Respir Physiol* 17: 365-385, 1973.
12. Hughes JMB, Rosenzweig DY, and Kivitz PB. Site of airway closure in excised dog lungs: histologic demonstration. *J Appl Physiol* 29: 340-344, 1970.
13. Macklem PT, Woolcock AJ, Hogg C, Nadel JA, and Wilson NJ. Partitioning of pulmonary resistance in the dog. *J Appl Physiol* 26: 798-805, 1969.
14. Mead J, Takishima T, and Leith D. Stress distribution in lungs: a model of pulmonary elasticity. *J Appl Physiol* 28: 596-608, 1970.

15. Milic-Emili J. Topographical inequality of ventilation. In: The Lung, edited by Crystal RG, West JB, Weibel ER, and Barnes PJ. Philadelphia PA: Lippincott-Raven, 1997, p. 1415-1423.
16. Muscedere JG, Mullen JBM, Gan K, Bryan AC, and Slutsky AS. Tidal ventilation at low airway pressure can augment lung injury. *Am J Respir Crit Care Med* 149: 1327-1334, 1994.
17. Robertson B. Lung surfactant. In: *Pulmonary surfactant*, edited by Robertson B, Van Goulde L, Batenburg J. Amsterdam: Elsevier, 1984.
18. Robertson PC, Anthonisen NR, and Ross WRD. Effect of inspiratory flow on regional distribution of inspired gas. *J Appl Physiol* 26: 438-443, 1969.
19. Saetta M, Ghezzo H, Kim WD, King M, Angus GE, Wang NS, and Cosio MG. Loss of alveolar attachments in smokers. *Am Rev Respir Dis* 132: 894-900, 1985.
20. Saetta M, Baraldo S, Corbino L, Turato G, Braccioni F, Rea F, Cavallesco G, Tropeano G,Mapp CE, Maestrelli P, Ciaccia A, Fabbri LM. CD8+ve cells in the lungs of smokers with chronic obstructive pulmonary disease. *Am J Respir Crit Care Med* 1999; 160: 711-717.
21. Salazar E, and Knowles JH. An analysis of the pressure-volume characteristics of the lung. *J Appl Physiol* 19: 97-104, 1964.
22. Stamenovic D, and Smith JC. Surface forces in lungs. II Microstructural mechanics and lung stability. *J Appl Physiol* 60: 1351-1357, 1986.
23. Stamenovic D, and Wilson T. Parenchymal stability. *J Appl Physiol* 73: 596-602, 1992.
24. Taskar V, John J, Evander E, Wollmer P, Robertson B, and Jonson B. Healthy lungs tolerate repetitive collapse and reexpansion. *Acta Anaesthesiol Scand* 39: 370-376, 1995.
25. Taskar V, John J, Evander E, Robertson B, and Jonson B. Surfactant dysfunction makes lungs vulnerable to repetitive collapse and reexpansion. *Am J Respir Crit Care Med* 155: 313-320, 1997.
26. Thurlbeck WM. Internal surface area and other measurements in emphysema. *Thorax* 22: 483-496, 1967.
27. Tschumperlin DJ, Oswari J, and Marguleis AS. Deformation-induced injury of alveolar epithelial cells. Effect of frequency, duration, and amplitude. *Am J Respir Crit Care Med* 162: 357-362, 2000.
28. Vlahakis NE, Schroder MA, Limper AH, and Hubmayr RD. Stretch induced cytokine release by alveolar epithelial cells in vitro. *Am J Physiol Lung Cell Mol Physiol* 277: L167-L173, 1999.
29. Young SL, Tierney DF, and Clements JA. Mechanisms of compliance change in excised rat lungs at low transpulmonary pressure. *J Appl Physiol* 29: 780-785, 1970.
30. Wyszogrodski I, Kyei-Aboagye E, Taeusch HW, and Avery ME. Surfactant inactivation by hyperventilation: conservation by end-expiratory pressure. *J Appl Physiol* 83: 461-466, 1975.

LEGENDS

Fig.1. Ensemble average of records of flow (V'), volume changes (ΔV), and tracheal pressure (Ptr) from ten consecutive breath cycles during baseline ventilation with PEEP of 2.3 cmH_2O ($PEEP_1$) and after 3 h ventilation on ZEEP ($ZEEP_2$) in two representative open-chest rabbits ventilated with high (**a**) and low inflation flows (**b**). Since inflation flow was constant, Ptr traces during inflation reflect dynamic pressure-volume relationships.

Fig. 2. Average relationship between volume above resting lung volume (ΔV) and quasi-static transpulmonary pressure (Pst) obtained during ventilation with PEEP of 2.3 cmH_2O before ($PEEP_1$) and after 3-4 h of ventilation on ZEEP ($PEEP_2$), and during the initial ($ZEEP_1$) and final period ($ZEEP_2$) of ventilation on ZEEP (see key to symbols) in 9 open chest rabbits ventilated with high (**Group A**) and low inflation flow (**Group B**), and in 6 open chest rabbits (**Group C**) ventilated with high inflation flow during ventilation with PEEP before ($PEEP_1$) and after 3-4 h of ventilation on PEEP ($PEEP_2$). Bars: SE. On PEEP, all data fit a unique mono exponential function.

Fig. 3. Relationships of additional lung resistance (ΔR) to duration of inflation obtained at an inflation volume of 11 $ml \cdot kg^{-1}$ during ventilation with PEEP of 2.3 cmH_2O before ($PEEP_1$) and after 3-4 h of ventilation on ZEEP ($PEEP_2$), at the beginning ($ZEEP_1$) and end of the 3-4 h period ($ZEEP_2$) of ventilation on ZEEP (see key to symbols) in 9 open chest rabbits ventilated with high (**Group A**) and low (**Group B**) inflation flow, and in 6 open chest rabbits (**Group C**) ventilated with high inflation flow during ventilation with PEEP before ($PEEP_1$) and after 3-4 h of ventilation on PEEP ($PEEP_2$). Bars: SE. Under all conditions, the data fit a monoexponential function.

Fig. 4. Relationship of changes in viscoelastic resistance to those in static elastance occurring after 10 min ($ZEEP_1$) and 3-4 h ($ZEEP_2$) of ventilation on ZEEP (see key to symbols), both expressed relative to the corresponding values during initial period of ventilation with PEEP of 2.3 cmH_2O ($PEEP_1$). Results obtained in 18 open chest rabbits ventilated with high or low inflation flows.

Fig. 5. Microphotographs of alveolar walls from a rabbit ventilated with low inflation flow (panel **A**) and a rabbit ventilated with high inflation flow (panel **B**). Arrows indicate polimorphonuclear leukocytes. Hematoxylin-eosin staining. Original magnification 800X.

Fig. 6. Microphotographs showing a bronchiole with a low percentage of abnormal alveolar attachments (panel **A**) and a bronchiole with a high percentage of abnormal alveolar attachments (panel **B**). Arrows indicate abnormal alveolar attachments. Hematoxylin-eosin staining. Original magnification 250X.

.

Table 1. Pa_{O_2}, Pa_{CO_2} and pHa, and wet-to-dry ratio of the lung of *group A* (high inflation flow), *B* (low inflation flow), and *C* rabbits (high inflation flow, no ZEEP ventilation)

	n		Pa_{O_2} mmHg	Pa_{CO_2} mmHg	pHa	wet/dry
Group A	9	$PEEP_1$	98±7	43.1±3.5	7.33±0.02	
		$ZEEP_1$	70±5*	50.1±3.3*	7.27±0.02*	
		$ZEEP_2$	82±6*†	51.1±4.3*	7.21±0.03*	
		$PEEP_2$	106±5	41.9±3.1	7.34±0.04	4.76±0.25
Group B	9	$PEEP_1$	90±8	46.4±3.9	7.32±0.04	
		$ZEEP_1$	71±6*	51.3±3.6*	7.29±0.02*	
		$ZEEP_2$	87±6*‡	51.8±3.5*	7.21±0.03*	
		$PEEP_2$	99±9	44.0±3.1	7.30±0.05	4.73±0.23
Group C	7	$PEEP_1$	96±6	43.5±1.3	7.34±0.02	
		$PEEP_2$	95±10	42.1±1.0	7.31±0.03	4.76±0.07

Values are means±SE. Pa_{O_2}, Pa_{CO_2}, and pHa: arterial P_{O_2}, P_{CO_2}, and pH, respectively; $PEEP_1$, ventilation with positive end-expiratory pressure (PEEP) of 2.3 cmH_2O at the beginning of the experiment; $ZEEP_1$ and $ZEEP_2$, initial and final part of the 3-4 h period of ventilation on zero end-expiratory pressure (ZEEP); $PEEP_2$, ventilation with PEEP after 3-4 h of ventilation either on ZEEP (*groups A* and *B*) or PEEP (*group C*). n, number of animals. Significantly different from corresponding values on $PEEP_1$, *P<0.001; significantly different from corresponding values on $ZEEP_1$, †P<0.05 and ‡ P<0.01.

Table 2. ΔP/Δt of *group A* (high inflation flow), *B* (low inflation flow), and *C* rabbits (high inflation flow, no ZEEP ventilation) during $PEEP_1$, $ZEEP_1$, $ZEEP_2$, and $PEEP_2$

	ΔP/Δt $cmH_2O \cdot s^{-1}$		ΔP/Δt $cmH_2O \cdot s^{-1}$
Group A			
$PEEP_1$	21.6±2.0	$ZEEP_1$	56.2±4.3§
$PEEP_2$	32.5±2.7†	$ZEEP_2$	89.3±6.3‡§
Group B			
$PEEP_1$	2.7±0.1	$ZEEP_1$	5.5±0.2§
$PEEP_2$	3.2±0.2*	$ZEEP_2$	8.6±0.3‡§
Group C			
$PEEP_1$	22.4±2.2		
$PEEP_2$	22.1±2.6		

Values are means±SE. ΔP/Δt mean rate of transpulmonary pressure changes during the first 90 ms of inflation; $PEEP_1$, ventilation with positive end-expiratory pressure (PEEP) of 2.3 cmH_2O at the beginning of the experiment; $ZEEP_1$ and $ZEEP_2$, initial and final part of the 3-4 h period of ventilation on zero end-expiratory pressure (ZEEP); $PEEP_2$, ventilation with PEEP after 3-4 h of ventilation either on ZEEP (*groups A* and *B*) or PEEP (*group C*). n, number of animals. * $P<0.01$ and † $P<0.001$ $PEEP_2$ vs $PEEP_1$ values; ‡ $P<0.001$ $ZEEP_2$ vs $ZEEP_1$ values; § $P<0.001$ ZEEP vs corresponding PEEP values.

Table 3. Values of constants in equation $V_o \cdot (1-e^{-K \cdot Pst})$ used to fit the lung inflation volume-pressure curve and ΔEELV during $PEEP_1$ and $PEEP_2$ in group A (high inflation flow), B (low inflation flow) and C rabbits (high inflation flow, no ZEEP ventilation)

		V_o ml	K cm H_2O^{-1}	ΔEELV ml
Group A				
	$PEEP_1$	83.1±3.6	0.184±0.007	26.9±1.9
	$PEEP_2$	82.7±4.0	0.181±0.010	27.3±2.2
Group B				
	$PEEP_1$	72.8±1.9	0.194±0.011	25.2±2.3
	$PEEP_2$	75.1±2.2	0.195±0.008	26.1±1.9
Group C				
	$PEEP_1$	78.0±3.8	0.167±0.010	25.1±2.6
	$PEEP_2$	77.2±4.3	0.175±0.010	27.9±3.5

Values are means±SE. V_o, maximum volume above resting lung volume; K, shape factor; ΔEELV, difference between end-expiratory and resting volume.

Table 4. Values of Est and Rint of *group A* (high inflation flow), *B* (low inflation flow), and *C* rabbits (high inflation flow, no ZEEP ventilation) during $PEEP_1$, $ZEEP_1$, $ZEEP_2$, and $PEEP_2$

	Est	Rint		Est	Rint
	$cmH_2O \cdot l^{-1}$	$cmH_2O \cdot s \cdot l^{-1}$		$cmH_2O \cdot l^{-1}$	$cmH_2O \cdot s \cdot l^{-1}$
Group A					
$PEEP_1$	131±8	14±1	$ZEEP_1$	381±20*†	34±3*†
$PEEP_2$	160±16	26±3*	$ZEEP_2$	460±22*†	69±7*†
Group B					
$PEEP_1$	143±7	15±1	$ZEEP_1$	328±15*†	24±2*†
$PEEP_2$	162±14	20±1*	$ZEEP_2$	401±17*†	52±3*†
Group C					
$PEEP_1$	143±6	13±1			
$PEEP_2$	152±9	13±1			

Values are means±SE. Est, quasi-static elastance; Rint, interrupter resistance. *Significantly different from values on $PEEP_1$ ($P<0.01$); † significantly different from corresponding values on PEEP ($P<0.01$).

Table 5. Values of Rvisc and τvisc computed according to Eq.1 of *group A* (high inflation flow), *B* (low inflation flow), and *C* rabbits (high inflation flow, no ZEEP ventilation) during $PEEP_1$, $ZEEP_1$, $ZEEP_2$, and $PEEP_2$

	Rvisc	τvisc		Rvisc	τvisc
	$cmH_2O \cdot s \cdot l^{-1}$	s		$cmH_2O \cdot s \cdot l^{-1}$	s
Group A					
$PEEP_1$	56±9	1.33±0.09	$ZEEP_1$	153±29*†	1.32±0.20
$PEEP_2$	59±11	1.29±0.12	$ZEEP_2$	182±35*†	1.24±0.15
Group B					
$PEEP_1$	59±4	1.18±0.11	$ZEEP_1$	117±15*†	1.23±0.17
$PEEP_2$	61±6	1.13±0.11	$ZEEP_2$	167±28*†	1.21±0.15
Group C					
$PEEP_1$	60±5	1.29±0.08			
$PEEP_2$	60±7	1.22±0.04			

Values are means±SE. Rvisc, viscoelastic resistance; τvisc, viscoelastic time constant. *Significantly different from values on $PEEP_1$ ($P<0.01$); † significantly different from corresponding values on PEEP ($P<0.01$).

Table 6. Indices of parenchymal damage, abnormal alveolar-bronchiolar coupling, and inflammation in lungs subjected to 3-4 h of ventilation with high (*group A*) or low inflation flow (*group B*) on ZEEP and with high inflation flow on PEEP only (*group C*)

	N	Lm μm	A-A %	D μm	Cells mm^{-1}
Group A	7	142 (107-163)	33.2† (29.2-35)	137 (102-182)	1*† (0.82-2.6)
Group B	7	145 (93-185)	31.3† (29-34.6)	124 (94-128)	0.79† (0.6-1)
Group C	5	162 (126-225)	7.2 (3.5-10.2)		0.14 (0.1-0.21)

Values are medians with range in parentheses. Lm, mean linear intercept; A-A, percentage of abnormal alveolar-bronchiolar attachments; D, distance between alveolar-bronchiolar attachments; Cells, number of polymorphonuclear leukocytes per unit length of alveolar septa. *P<0.05 *group A* vs *B*; †P<0.01 *groups A* and *B* vs *C*.

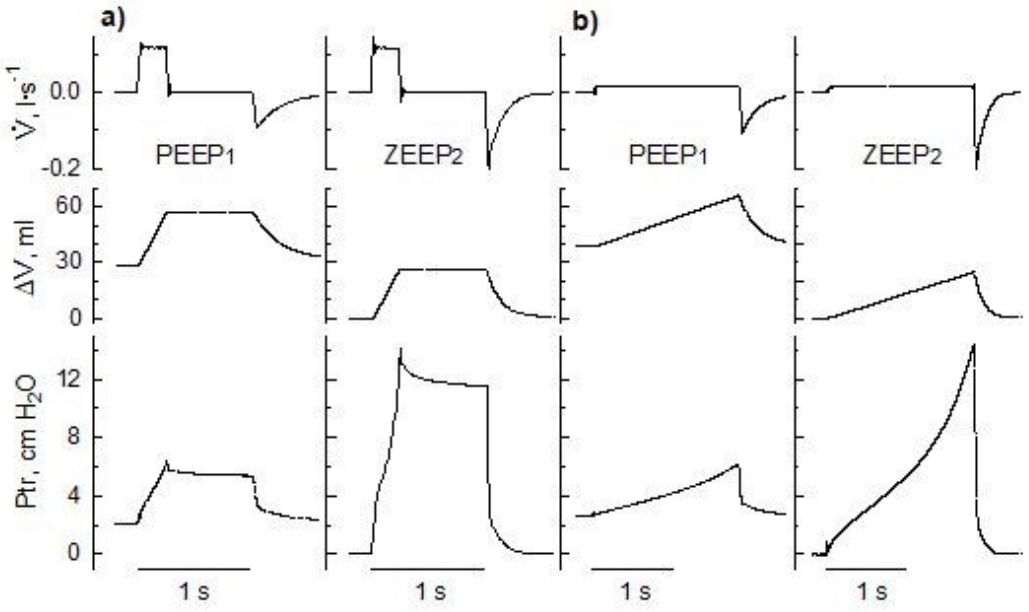
a)
b)
$\dot{V}_I$, l·s^{-1}
0.0
-0.2
PEEP1
ZEEP2
PEEP1
ZEEP2
ΔV, ml
60
30
0
Ptr, cm H2O
12
8
4
0
1 s
1 s
1 s
1 s

Figure 1

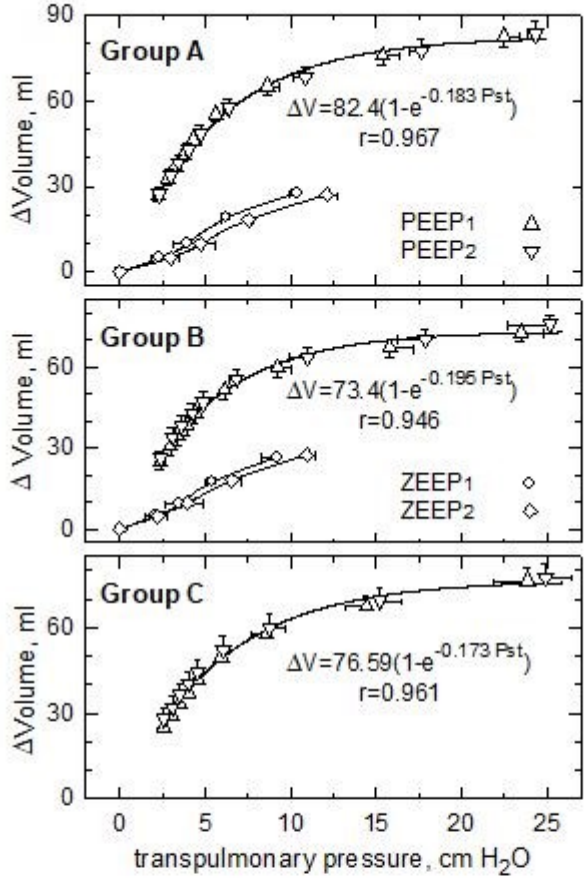
Group A
ΔV=82.4(1-e^-0.183 Pst)
r=0.967
PEEP1
PEEP2
Group B
ΔV=73.4(1-e^-0.195 Pst)
r=0.946
ZEEP1
ZEEP2
Group C
ΔV=76.59(1-e^-0.173 Pst)
r=0.961
ΔVolume, ml
Δ Volume, ml
transpulmonary pressure, cm H2O

Figure 2

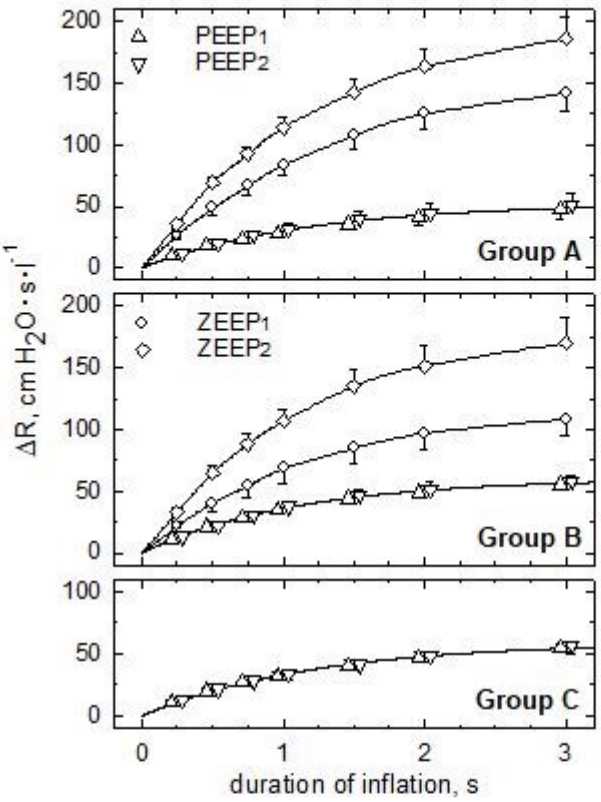
PEEP1
PEEP2
Group A
ZEEP1
ZEEP2
Group B
Group C
ΔR, cm H2O·s·l-1
duration of inflation, s
0
50
100
150
200
1
2
3

Figure 3

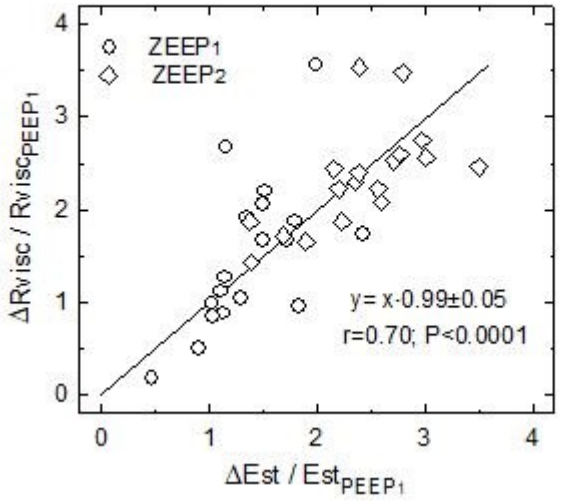
ZEEP1
ZEEP2
y= x-0.99±0.05
r=0.70; P<0.0001
ΔRvisc / RviscPEEP1
ΔEst / EstPEEP1
0
1
2
3
4

Figure 4

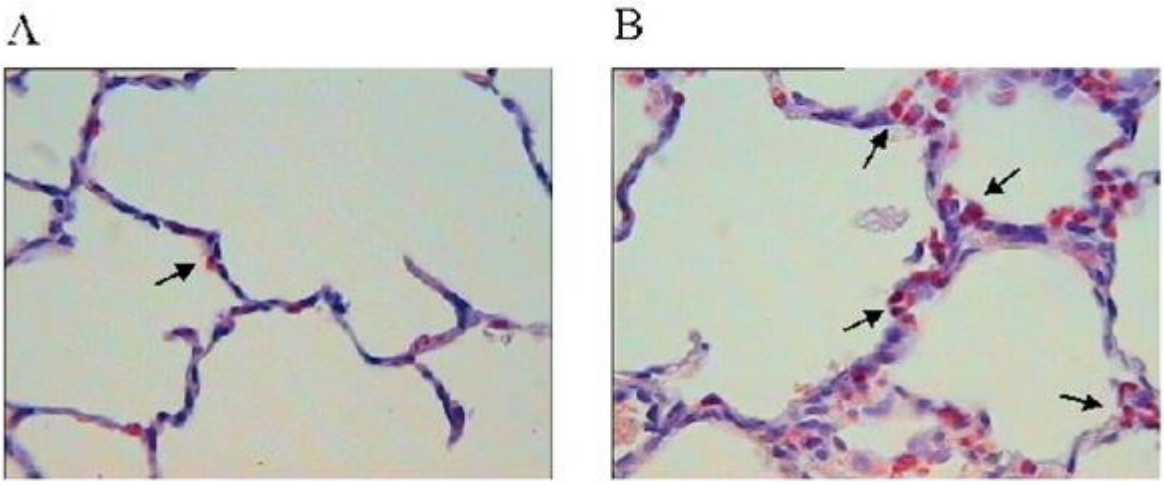

Figure 5

A

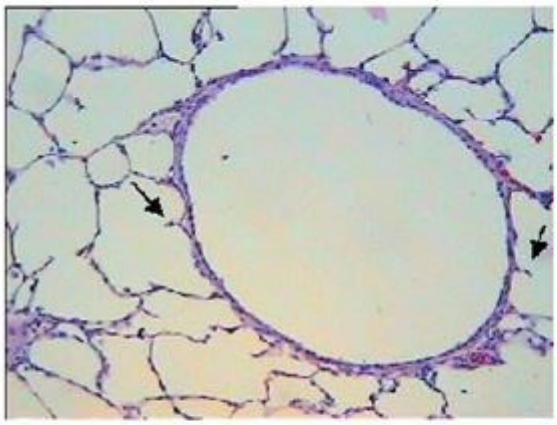

B

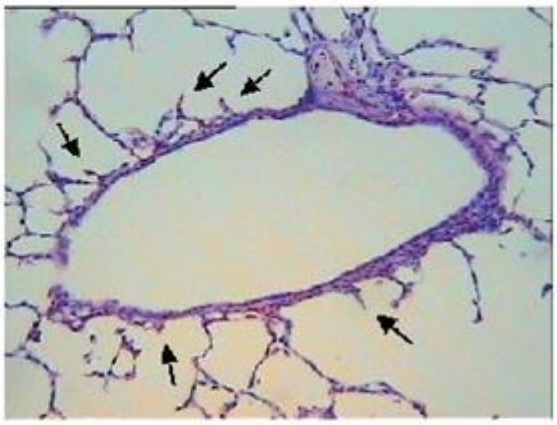

Figure 6